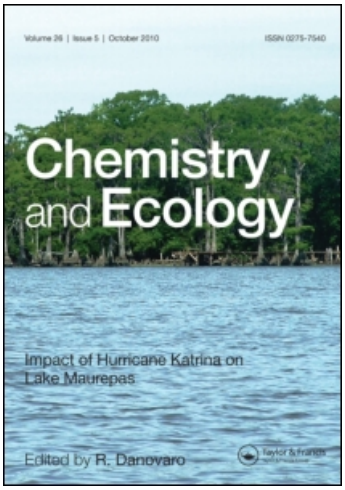

Chemistry and Ecology
Publication details, including instructions for authors and subscription information:
http://www.informaworld.com/smpp/title~content=t713455114

Analysis of mesoscale productivity processes in the Adriatic Sea: Comparison between data acquired by Sarago, a towed undulating vehicle, and CTD casts

Viviana Piermattei[a]; Giovanni Bortoluzzi[b]; Stefano Cozzi[c]; Antonia Di Maio[a]; Marco Marcelli[a]
[a] University of Tuscia, DECOS, Viterbo, Italy [b] CNR ISMAR, Bologna, Italy [c] CNR ISMAR, Trieste, Italy

To cite this Article Piermattei, Viviana , Bortoluzzi, Giovanni , Cozzi, Stefano , Maio, Antonia Di and Marcelli, Marco(2006) 'Analysis of mesoscale productivity processes in the Adriatic Sea: Comparison between data acquired by Sarago, a towed undulating vehicle, and CTD casts', Chemistry and Ecology, 22: 4, S275 — S292
To link to this Article: DOI: 10.1080/02757540600757765
URL: http://dx.doi.org/10.1080/02757540600757765

Chemistry and Ecology
August 2006, Vol. 22 (Supplement 1), pp. S275–S292

Taylor & Francis
Taylor & Francis Group

Analysis of mesoscale productivity processes in the Adriatic Sea: Comparison between data acquired by Sarago, a towed undulating vehicle, and CTD casts

VIVIANA PIERMATTEI†, GIOVANNI BORTOLUZZI‡, STEFANO COZZI§, ANTONIA DI MAIO† and MARCO MARCELLI*†

†University of Tuscia, DECOS, via di S. Giovanni Decollato 1, 01100, Viterbo, Italy
‡CNR ISMAR, Via P. Gobetti, 101 40129 Bologna, Italy
§CNR ISMAR, Via Romolo Gessi, 2 34123 Trieste, Italy

(Received 30 May 2005; in final form 27 March 2006)

A modern approach to the study of pelagic ecosystems requires both an appropriate spatial and temporal resolution and a synoptic observation. For this reason, it is indispensable a rapid and high-resolution data acquisition along the water column. During the CNR project PRISMA II, four oceanographic cruises were performed in the Northern Adriatic Sea to analyse the high variability of ecological processes related to the frontal system. The SARAGO, a towed undulating vehicle, allowed a fine description of physical and biological acquired parameters (CTD, chlorophyll *a* concentration, photosynthetic efficiency, PAR). In succession, CTD and bottle carousel casts were performed to analyse physical and biogeochemical features. In this work, we compare the distribution and quantification of the relevant variables acquired by the two different sampling methods. A mathematical model was applied to estimate primary production.

Keywords: Adriatic Sea; Towed vehicle; Primary production

1. Introduction

The distribution of phytoplankton population in the marine environment is heterogeneous on both meso- and small scales [1]. The importance of the mesoscale processes on the dynamics of phytoplankton communities has been largely recognized, and Margalef [2] has observed that 'inside the mesoscale compartments there is much small-scale heterogeneity, usually studied along transects'.

Several processes and interactions concur to generate and maintain this heterogeneity. Hydrologic features of the water column, turbulence, vertical mixing, lateral transport, and irradiance levels determine the patchiness of phytoplankton in the sea [3]. These physical forcings influence the availability of nutrients, which are utilized by the phytoplankton, and the distribution of the cells in the water column.

*Corresponding author. Email: marcomarcell@tin.it

Chemistry and Ecology
ISSN 0275-7540 print/ISSN 1029-0370 online © 2006 Taylor & Francis
http://www.tandf.co.uk/journals
DOI: 10.1080/02757540600757765

As a result of the interaction between physical conditions and availability of resources, phytoplanktonic organisms modulate their physiological state and activity. These mechanisms are at the base of the productivity of marine ecosystems and should be studied using adequate sampling methods, capable of obtaining the necessary spatial resolution and synoptic view. The traditional methods used in oceanographic cruises are limited both in terms of the spatial and temporal sampling rate and in the duration of the observation.

CTD casts and bottle sampling cannot permit a detailed analysis of the marine environment at the phytoplankton scales, particularly in areas like the Northern Adriatic Sea that are subject to highly variable oceanographic conditions.

The development of remote sensing has more recently permitted synoptic observations on large areas. However, this approach to the study of marine ecosystems suffers to date from a low spatial resolution and the total absence of the third dimension, the depth [4].

A third approach to the oceanographic studies is the utilization of towed measuring devices [5], which permits a high sampling rate and a high spatial resolution, maintaining a quasi-synoptic temporal view [6–8]. Although it has not been commonly used to date, it seems to be the best way to study several marine areas [9, 10].

During the CNR PRISMA 2 Biogeochemical Cycles Research Project, four cruises, on the RV *Urania*, were carried out utilizing an undulating underwater vehicle, SARAGO [11], in order to describe the frontal system generated by continental runoff of low-salinity waters in the western area of the Northern Adriatic Sea [12].

The SARAGO vehicle has provided a quasi-synoptic measurement of several physical, chemical, and biological parameters in the water column, with a high vertical and horizontal resolution. In this work SARAGO data were compared with the data obtained by the traditional sampling in fixed stations.

The aim of this study is to describe the small-scale variability of some hydrological and biological properties in the western coastal waters of the Northern Adriatic Sea on the basis of the SARAGO data set. This variability is not emphasized by traditional sampling methods in fixed stations.

Moreover, the results presented in this study demonstrate, on a statistical basis and quantitative estimate, how much information/variability is lost passing from a 'continuous' undulating data acquisition vehicle (SARAGO) to a 'classic' data acquisition (CTD casts).

2. Materials and methods

2.1 *Investigated area*

Data were collected in two summer (U1 and U3 in June 1996 and 1997, respectively) and two winter (U2 and U4 in February 1997 and 1998) cruises on the RV *Urania*, during the PRISMA 2 Research Project. Two areas were studied: a northern area, located near the Po River Delta, and a southern area, located along the Italian cost between Senigallia and Ancona (figure 1).

Both areas are portions of the coastal front, generated by freshwater inputs into the basin, that characterized the western side of the Northern Adriatic Sea. This is formed by the low-salinity waters, generated by discharges of the Po River and of other local contributors along the Italian coast. The structure of this coastal front is strongly variable, as the spread of the low-salinity waters and the presence of vertical or horizontal density gradients depend on the continental runoffs and on their interaction with meteorological forcings and circulation on the basin scale.

Each survey was performed upon a two-way design: a fine characterization utilizing the SARAGO and subsequentely data collection and water sampling by traditional CTD casts in fixed stations.

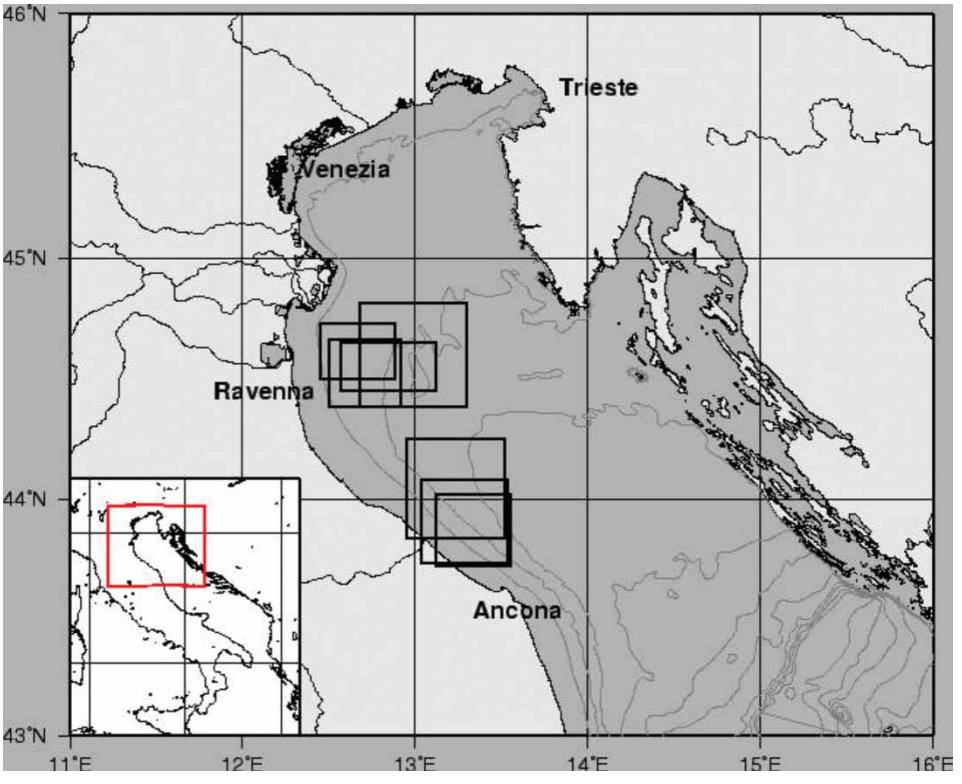

Figure 1. Left: Prisma 2 Project sampling areas. Right: Example of SARAGO routes and CTD stations in U2 south survey.

During the SARAGO surveys, at the beginning and at the end of every transect, intercalibration profiles between SARAGO, CTD, and Primprod 1.08 were made, and water bottles were sampled, in order to calibrate the instruments.

2.2 *Sarago*

SARAGO is an underwater undulating towed fish [11], whose present Mark was planned and carried out in 1990–1993 in the Ismes S.p.A. laboratories [13], able to work in the water column from depths of 0 to 300 m, along sinusoidal pre-programmed trajectories (figure 2).

Inside the vessel, control instruments (pressure transducer, inclinometers, and echosounder) ensure the detection of the real trajectory followed in the water (figure 3). During Prisma 2, the payload of SARAGO consisted of a SBE 19, to measure CTD and O_2 and a double impulse fluorometer Primprod 1.11, to measure irradiance (PAR), chlorophyll *a* and photosynthetic efficiency. The SARAGO towing speed was about 6 knots, and the acquisition rate was two samples per second.

The Primprod 1.11 is a submersible pump-and-probe fluorometer that derives from the similar fluorometer Primprod 1.08, developed at the Biophysic Institute of the Moscow University [14] (in agreement with Falkoskwy theories), described by Antal [15] (figure 4).

The functioning principle of the Primprod 1.11 is the same as that of the 1.08: the fluorometer generates sequential pump-and-probe flashes [15]. The first probing flash measures the fluorescence intensity (F_0) with open PS II centres; the saturating (pump) flash, 0.5 s after the first, that converts most of the RC to the closed state, measures Fl, fluorescence of

Figure 2. SARAGO vehicle in water.

chlorophyll *a*, like all other fluorometers; the second probing flash measures the fluorescence (F_{max}), which corresponds to the I1 level of fluorescence saturation [16] and that follows the pump flash after 50 μs, a time comparable to the reaction centre turnover time.

The Primprod 1.11 presents several technical changes with respect to the 1.08 probe:

- the water is conveyed from the prow of the vehicle to the measurement chamber by means of a hydraulic circuit controlled by a pump;
- the probe measures the second saturating flash, for comparison with other saturating fluorometers;
- the temperature sensor has a higher accuracy (0.01 °C vs. 0.1 °C);
- the probe can manage three further sensors, with a digital input and transmission system.

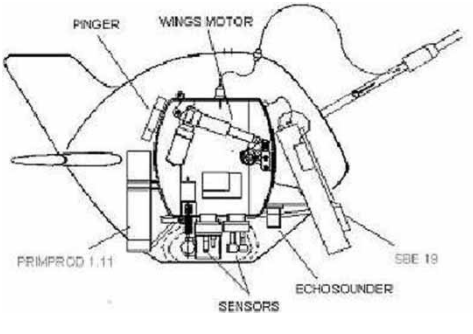

SARAGO characteristics	
Tow speed	1-10 Kn
Maximum Depth	standard 200, up to 300 m
Acquisition rate	1 - 3600 sec
Weight (air)	150 Kg
Weight (water)	70 Kg
Dimensions (LxWxH)	1.3 m x 1.4 m x 0.8 m
Materials	Pressure case and frame SS AISI 316, reinforced fiberglass

Figure 3. Left: Section of SARAGO vehicle. Right: SARAGO main characteristics.

Figure 4. Primprod 1.11 probe.

The PrimProd 1.11 fluorescence data were calibrated by means of orthogonal regression with chlorophyll *a* values obtained from water samples collected using a standard G.O. 1016 I, 10-litre 24 Niskin bottle carousel. Chlorophyll *a* in the water samples was measured utilizing fluorometric standard methods [17, 18] (figure 5).

2.3 *CTD casts*

The SBE 911 plus CTD profiler measured temperature, salinity, pressure, oxygen and density in fixed stations. It was equipped with a Sea Tech Fluorometer, to measure chlorophyll *a* saturated

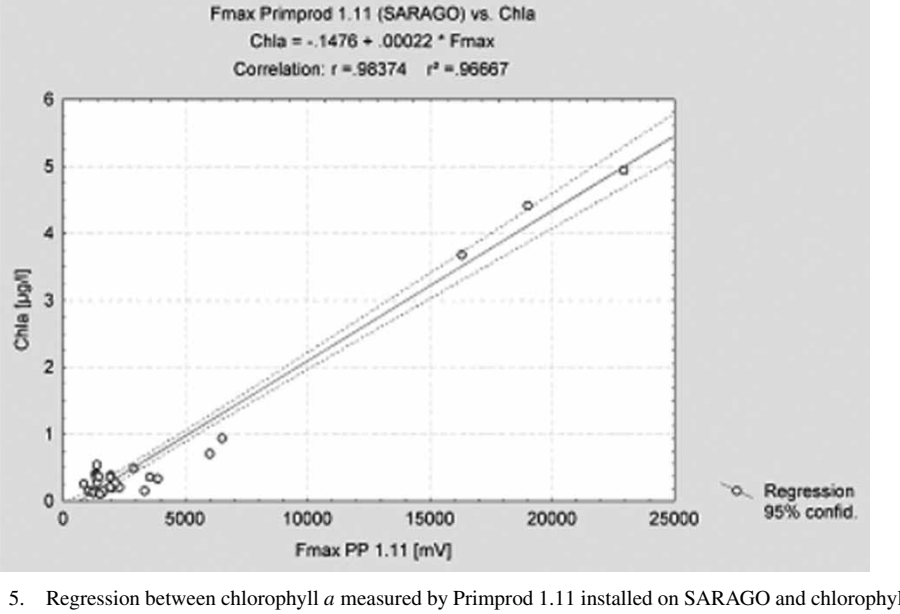

Figure 5. Regression between chlorophyll *a* measured by Primprod 1.11 installed on SARAGO and chlorophyll *a* measured in the laboratory by the spectrofluorometric method. Data refer to intercalibration stations.

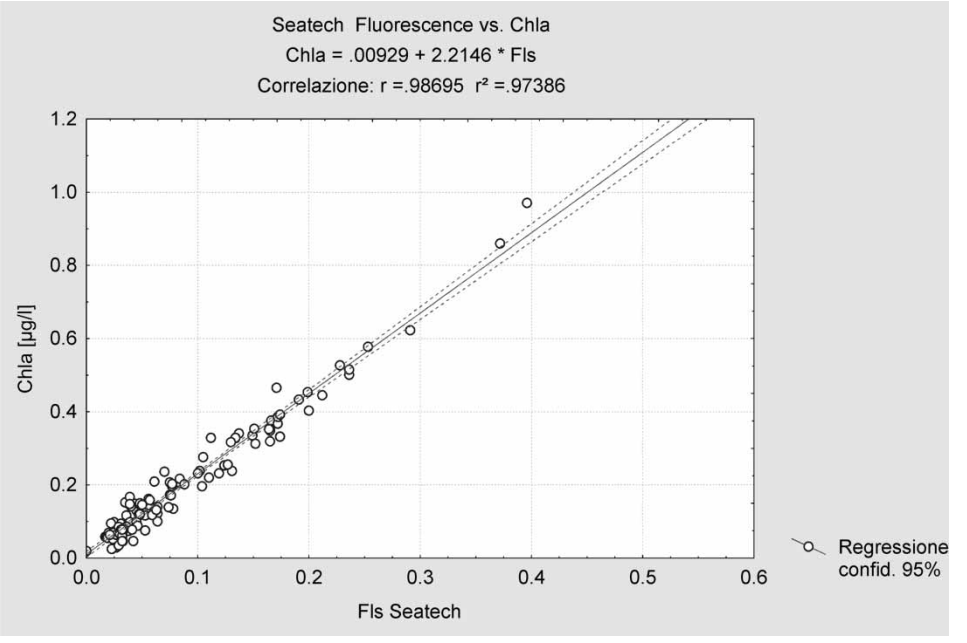

Figure 6. Regression between chlorophyll *a* measured by Seatech and chlorophyll *a* measured in laboratory by the spectrofluorometric method.

fluorescence, to calculate phytoplankton biomass. CTD data were processed by Seasoft. The water sampling were performed with a 24 standard Niskin bottle (10 litre) carousel (figure 6).

2.4 *Spatial analysis*

The first step in understanding ecological processes is to identify patterns [19], because many processes, like phytoplankton patches, operate on different scales. In order to describe the spatial patterns and to characterize the spatial variability, we applied experimental variograms, which estimate the semivariance function $\gamma(h)$. This gives a measure of spatial correlation between data, describing their relation with distance and direction [20].

The semivariance value is a function of the distance that separates points in the space, h, the so-called LAG distance. The semivariance increases with the increase in distance, h, indicating the differences between the $Z(x)$ values with increasing distances.

Sperimental variograms, $\gamma^*(h)$, are calculated [21] as:

$$\gamma^*(h) = \left\langle \sum_{N(h)} [Z(x_i + h) - Z(x_i)]^2 \right\rangle / 2\,N(h).$$

The square of the differences is calculated for all the possible pairs of points, which are distant between them h, with N the number of data.

On the variogram diagram, each point displays the value of a measure of spatial variability between pairs for the corresponding magnitude of a separation vector h [22].

The variogram model would have to start from the axes origin (where the model intercepts the y-axis), because when the distance is $h = 0$, the values of points have no difference. Nevertheless, we have to consider a component of uncertainty that causes a model shift from the origin; this shift is called the *nugget effect*.

The nugget effect quantifies the sampling and assaying errors, and the scale variability (*i.e.* spatial variation occurring at distance closer than the sample spacing) and makes it possible to determine whether the sampling method coincides with the real spatial and temporal extension of the studied phenomena.

In order to represent the distribution of hydrological and biological parameters, we used the Kriging interpolation method, a geostatistical gridding method, that produces visually appealing maps from irregularly spaced data, based on the linear variogram [23]. This method allows interpolation of the values of the available variables to obtain an estimation of the values in the areas with lack of data and thus emphasizes the local spatial structure of the variable.

Otherwise, this method is based on an empirical semivariogram that changes the distribution of values from discontinuous to continuous and does not consider the real variance of the estimated values. For these reasons, the estimation of the local variance obtained by Kriging interpolation is biased, and therefore the data set is not suitable for statistical hypothesis tests.

2.5 *Primary production*

Primary production was calculated by a first version of the Phyto VFP model [24, 25]. The model uses vertical distribution of biomass, PAR level, and photosynthetic efficiency to calculate the punctual phytoplanktonic primary production (mgC m^{-3} h^{-1}). The model also estimates primary production for the unit of area (mgC m^{-2} h^{-1}), by integration of the punctual values, from surface to photic depth, and simulates the P–I curve (figure 7), subdividing the water column in three regions, as a function of fixed PAR values, experimentally calculated as follows:

(1) a photo-limited region, where the production increases linearly with light:

$$P = \phi \cdot a^* \cdot I \cdot \text{Chl } a \cdot \frac{F_v}{F_{\max}};$$

(2) a photo-saturated region, where the production is constant:

$$P = \phi \cdot a^* \cdot E_k \cdot \text{Chl } a \cdot \frac{F_v}{F_{\max}}; \text{ and}$$

(3) a photo-inhibited region, where the production decreases in inverse proportion to light:

$$P = \frac{\phi \cdot a^* \cdot E_k \cdot E_I \cdot \text{Chl } a \cdot \frac{F_v}{F_{\max}}}{I};$$

where P = primary production; ϕ = quantum yield of the photosynthetic process, 0.1 molC 10 mol photon^{-1} [26]; a^* = specific absorption coefficient of the phytoplankton per

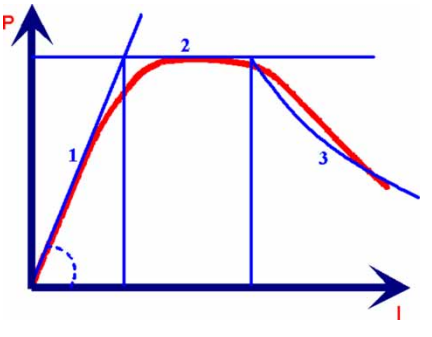

Figure 7. P–I curve divided into three regions.

mg chlorophyll a m^{-3}, expressed in m^2 mg chlorophyll, a^{-1}, 0.016 m^2 mg Chl a^{-1} [27]; I = irradiance (PAR); E_k = maximum irradiance value, equivalent to the maximum of photosynthetic efficiency; E_I = irradiance value at the beginning of the photo-inhibition area.

The E_k and E_I values utilized in the model for this work were obtained by measurements carried out in the Adriatic Sea [28]. The primary production estimated values were compared with ^{14}C measurements of primary production obtained with standard methods [29] (figure 8).

2.6 *Quantification*

To compare further SARAGO and CTD cast data, a fine quantitative estimation of the abundance of chlorophyll a has been performed.

We selected several transects where the CTD stations and SARAGO routes are superimposed. For every transect we created, using the Kriging interpolation method, two maps with the same dimensions (depth and distance) and the same grid node number and distribution: one for SARAGO and one for CTD data. Every grid node corresponds to a chlorophyll a concentration value (mg m^{-3}). Every grid file therefore represents a depth (m)–distance (m)–chlorophyll a (mg m^{-3}) section.

Afterwards, we estimated the chlorophyll a quantities in all the grids, considering the variation of chlorophyll a concentration in the depth–distance section. Considering the section with a thickness of 1 m, we introduce the specific chlorphyll a concentration, that is the quantity of chlorophyll a per surface unit of section (mg m^{-2}), *i.e.* the distribution of chlorophyll a mass (mg) on the section (m^2).

Assuming that y is the depth (m), x is the distance (m), and $C(x, y)$ is the distribution function of the specific chlorophyll a (mg m^{-2}), we calculate the chlorophyll a quantity, $Q_{\text{Chl a}}$ (mg), as:

$$Q_{\text{Chl } a} = \int_{y_{\min}}^{y_{\max}} \int_{x_{\min}}^{x_{\max}} C(x, y)\, \mathrm{d}x\, \mathrm{d}y.$$

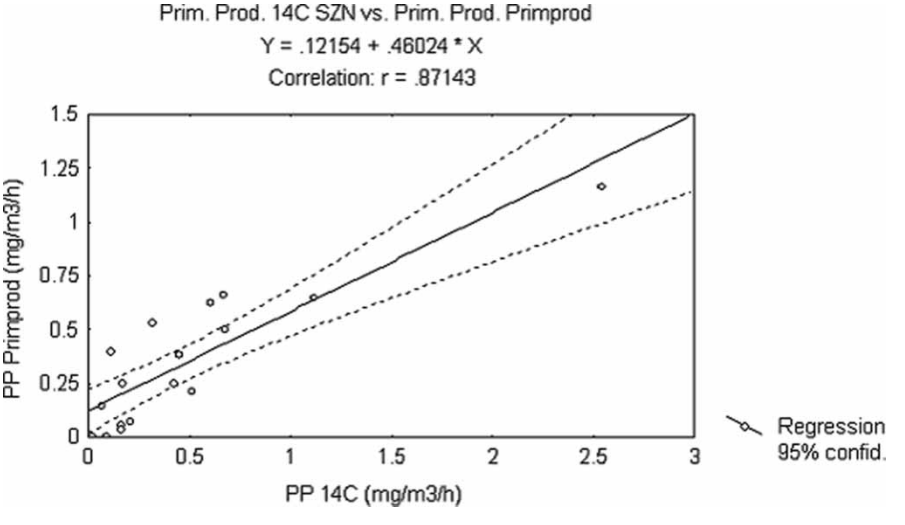

Figure 8. Regression between primary production estimated by Primprod 1.11 and primary production measured by the ^{14}C method.

In order to verify if the grid file, on which we calculated the chlorophyll *a* quantity, was dense enough, we compared the integral results with the other quantities, obtained by three different numerical integration algorithms: extended trapezoidal rule, extended Simpson's rule, and extended Simpson's 3/8 rule [30].

3. Results

In order to compare the two sampling methods, we analysed the temperature, salinity, and chlorophyll *a* of the SARAGO and CTD casts of some transects (figure 9), through vertical depth (m)–distance (nm) sections, with the Kriging interpolation method.

The representations of the variables demonstrate the presence and position of the frontal system. Between SARAGO and CTD cast surveys, there is a temporal interval that generates

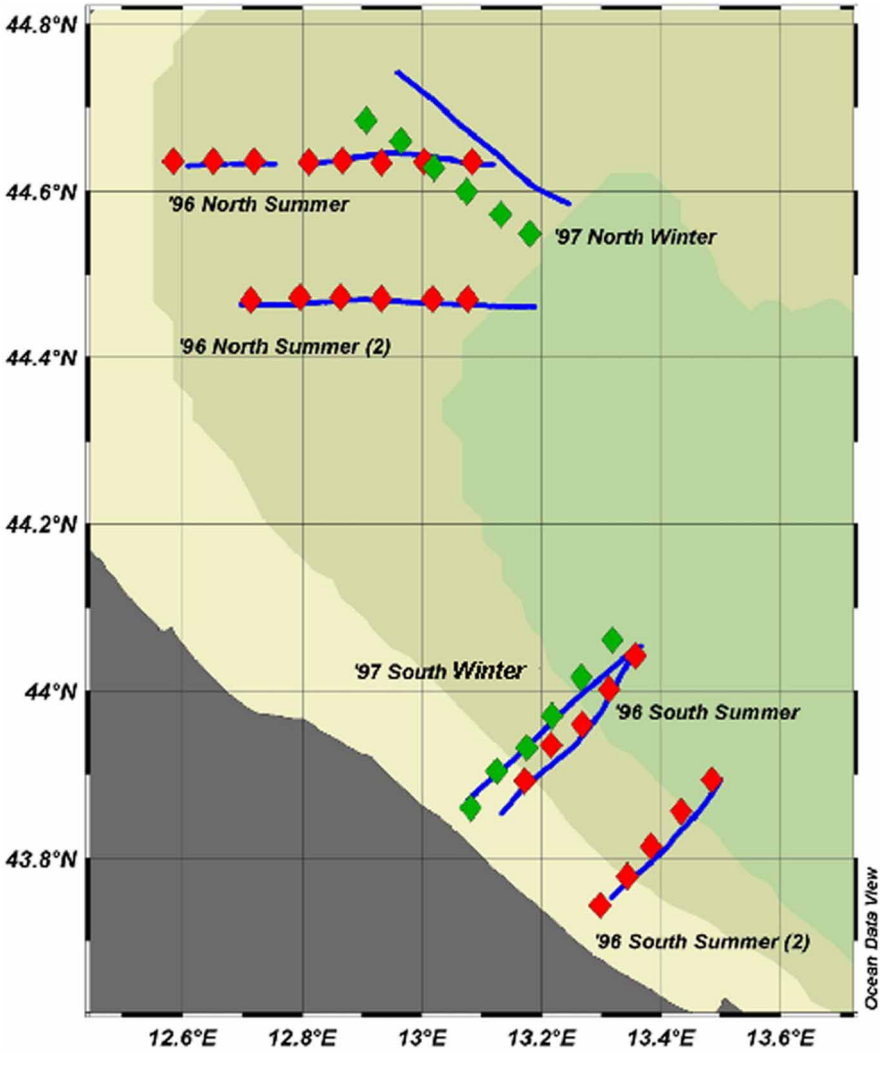

Figure 9. SARAGO and CTD analysed transects.

differences between the distribution of variables. In any case, the SARAGO sections always provide a better detail and resolution for the structures present in the study area, most of all in the distribution of chlorophyll *a*.

SARAGO data were intercalibrated with CTD cast data both for physical variables and for chlorophyll *a*. Among the analysed sections, we report three (figures 10–12) to show the aforementioned differences between SARAGO and CTD. All transects show the distribution of both sampling methods measure points: sinusoidal trajectories along the water column for SARAGO; vertical profiles in fixed station for CTD casts (figure 13).

The SARAGO data are much denser than CTD casts and consequently allow a higher spatial resolution. We obtained a SARAGO profile approximately every 350 m, while CTD casts have a profile about every 3 nm (5556 m). This means that for every CTD profile, there are about 16 SARAGO profiles. This very high spatial resolution represents the information better. It is particularly evident in the distribution of the chlorophyll *a*, that allows a fine description of patchiness with a higher degree of accuracy.

Another fundamental difference between the two sampling methods is due to the speed of transects realization: the SARAGO sections were performed in 2–3 h, with a speed of aboout 6–7 knots, while CTD cast sampling required a longer time (with a minimum of 4 h up to a maximum of 16 h).

The spatial and temporal resolution and the speed of the SARAGO method always permits the observation of the haline front with a high degree of accuracy. This resolution is not possible with the CTD casts, because of the high variability of the frontal system and of the low horizontal resolution of the sampling method.

The distribution of chlorophyll *a* is well described by SARAGO. If we enlarge parts of the sections, we can observe the patchiness distribution, allowing a measure of their wideness

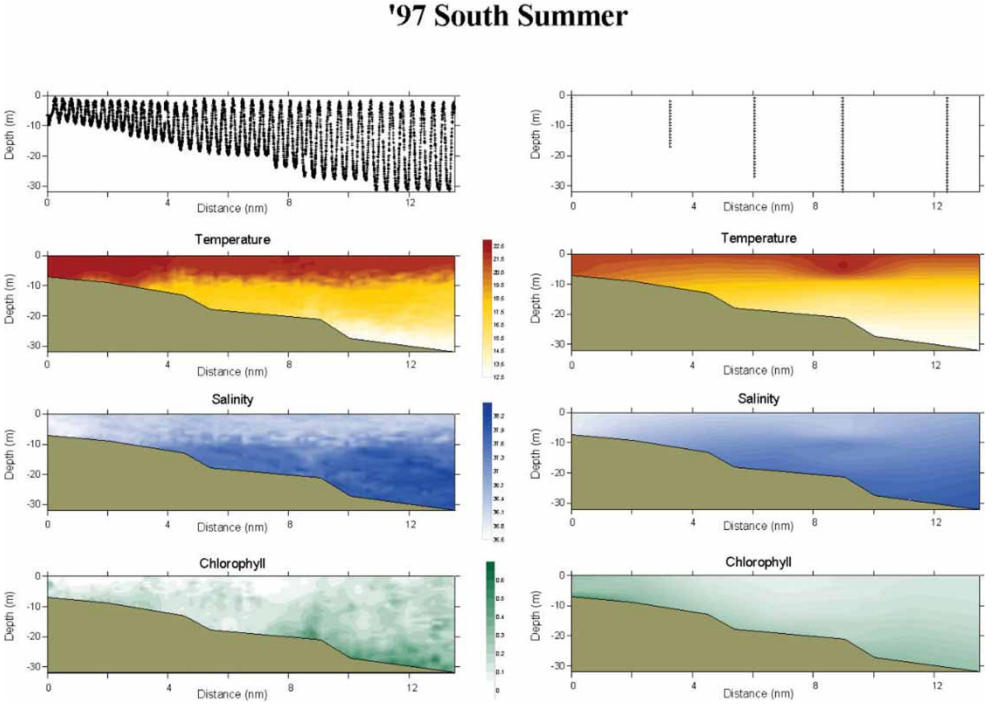

Figure 10. 1997 South Summer transect. Depth–distance sections. Top to bottom: SARAGO and CTD measure points; temperature (°C); salinity (PSU); chlorophyll *a* (mg l^{-1}).

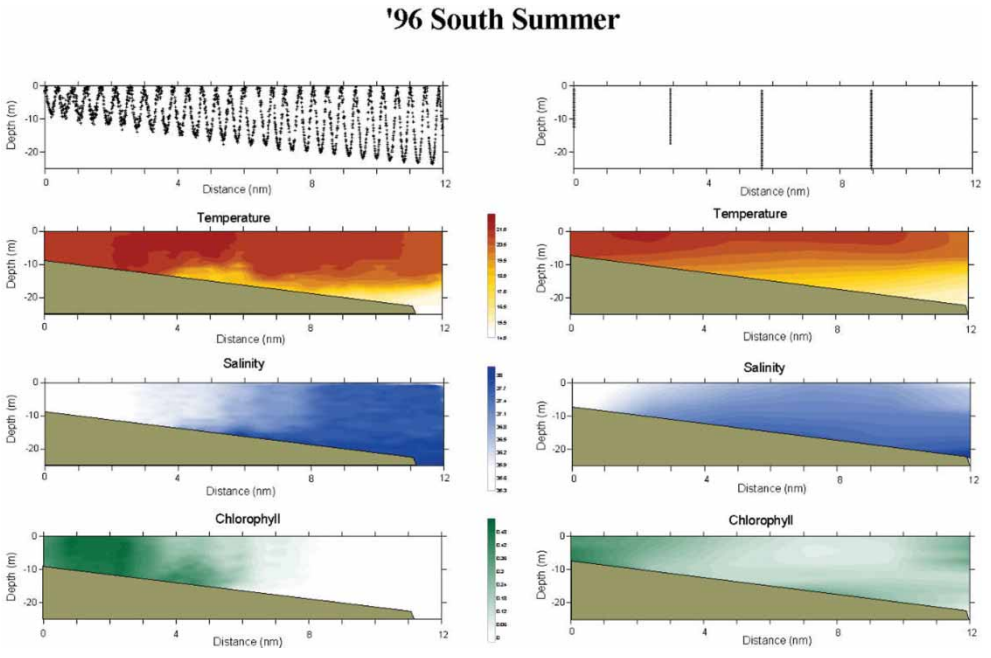

Figure 11. 1996 South Summer transect. Depth–distance sections. Top to bottom: SARAGO and CTD measure points; temperature (°C); salinity (PSU); chlorophyll *a* (mg l^{-1}).

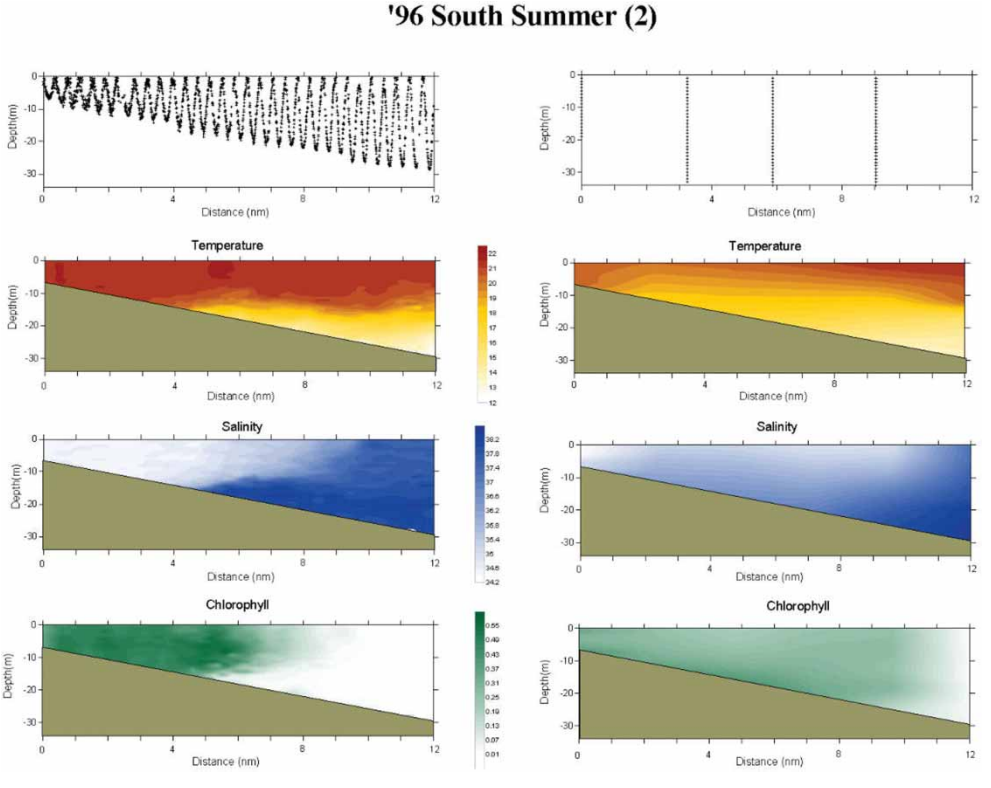

Figure 12. 1996 South Summer (2) transect. Depth–distance sections. Up to down: SARAGO and CTD measure points; temperature (°C); salinity (PSU); chlorophyll *a* (mg l^{-1} l^{-1}).

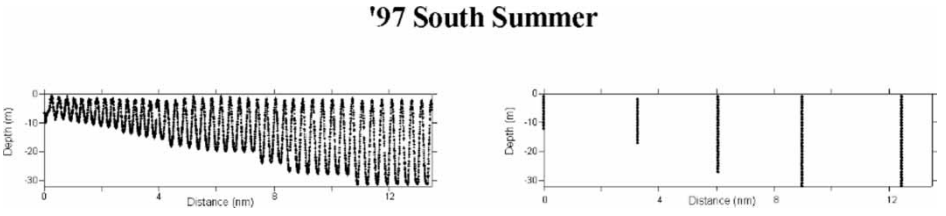

Figure 13. Acquired measure points. Left: SARAGO sinusoidal trajectories. Right: CTD casts.

(figure 14). The representation of these fine structures is completely absent in the interpolation of the CTD profiles (cf. figures 10–12).

In order to confirm the synopticity of the SARAGO method, we complete the work with a geostatistical analysis of the variables of interest, by means of variograms.

Data have been analysed through two statistic instruments, one that calculates a linear variogram model (Surfer 8) and the other a spherical model (GS + 5).

In this work, we present an example of the experimental variograms of temperature, salinity, and chlorophyll *a*, obtained by the analysis of the different SARAGO and CTD transects, calculated by a linear variogram (figure 15a–c); x is represented by the separation distance, y by the semivariance (section D 'Spatial analysis').

To compare the sampling scales coherence of the different methods we represent the nugget effect of SARAGO and CTD cast data. In the variogram diagrams, the nugget effect is represented by the distance between the model and the origin of the axes (where the model intercepts the y-axis). The nugget effect is a measure of the potential errors in the collection of the data. The errors may be due to a difference between the sampling and the phenomena scales, or may be due to measurement errors.

Table 1 shows the nugget effect values of temperature, salinity, and chlorophyll *a* of SARAGO and CTD data. The chlorophyll *a* nugget effects for the two sampling methods are compared in figure 16.

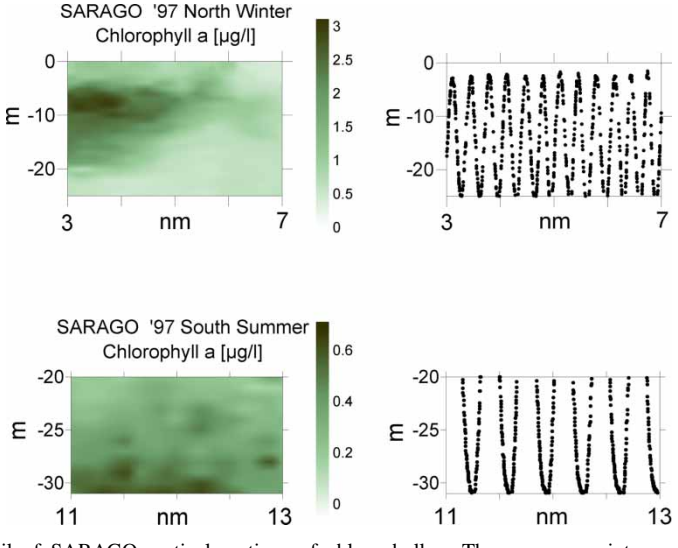

Figure 14. Detail of SARAGO vertical sections of chlorophyll *a*. The measure points cover the patchiness dimensions.

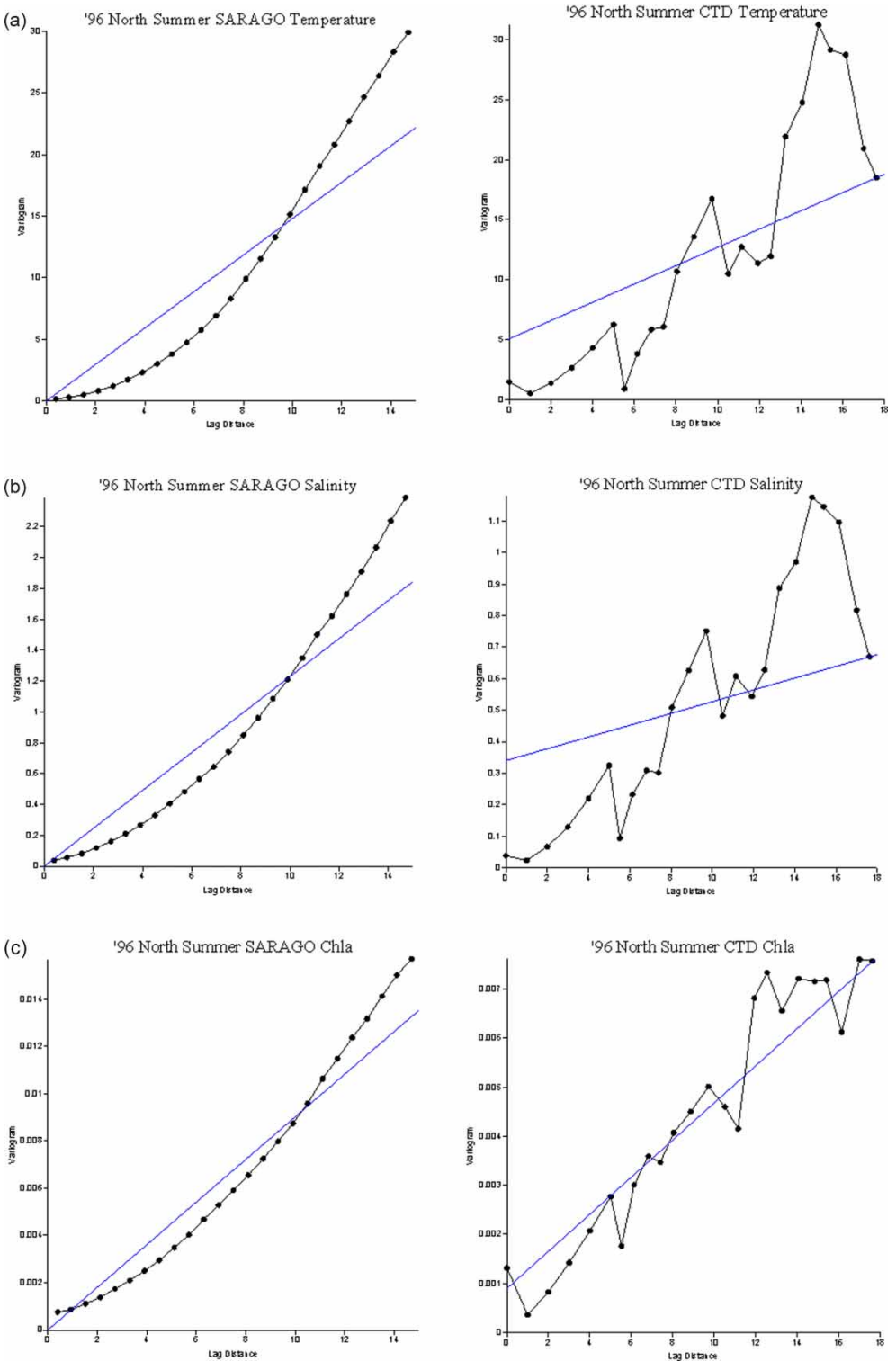

Figure 15. (a) SARAGO and CTD temperature (°C) variograms of the'96 North Summer transect. (b) SARAGO and CTD salinity (PSU) variograms of the'96 North Summer transect. (c) SARAGO and CTD chlorophyll *a* (μ g l^{-1}) variograms of the'96 North Summer transect.

Table 1. SARAGO and CTD temperature (°C), salinity (PSU), and chlorophyll *a* (μ g l^{-1}) nugget-effect values of the transects analysed.

NP	Transect	Temperature (°C)	Salinity (PSU)	Chlorophyll *a* (μ g l^{-1})
Sarago				
1	96 North Summer	0	0	0
2	96 South Summer	0	0	0
3	96 South Summer2	0	0	0
4	97 North Winter	0	0	0.0162
5	97 South Winter	0.061	0.0582	0.0383
6	97 South Summer	0	0	0.00419
CTD casts				
1	96 North Summer	2.25	0.34	0.000894
2	96 South Summer	0	0.011	0.0318
3	96 South Summer2	0	0	0.166
4	97 North Winter	0	0	0.57
5	97 South Winter	0.262	0.477	0.295
6	97 South Summer	0	0	0.0466

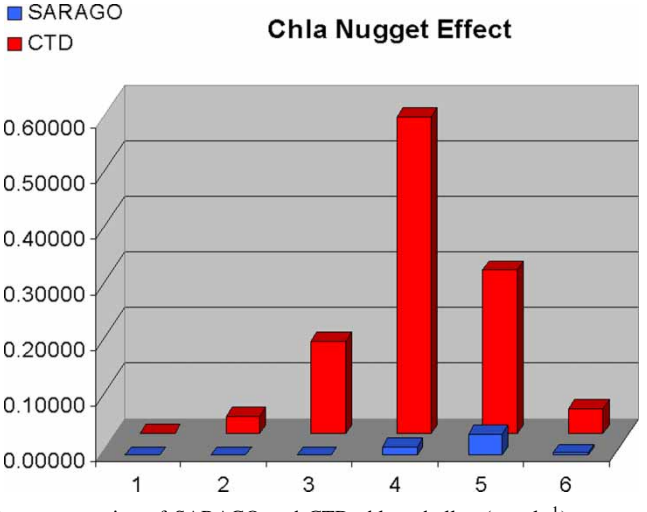

Figure 16. Graphic representation of SARAGO and CTD chlorophyll *a* (μ g l^{-1}) nugget effect values of the analysed transects.

We clearly see that the SARAGO data better represent the scales of the process. If there is a small difference in the description of the distribution of the hydrological variables, between SARAGO and CTD casts, there is a considerable difference in the representation of chlorophyll *a*. The lowest values of the nugget effect indicate a higher spatial autocorrelation and continuity in the SARAGO data.

Next, we present the results of the biomass quantity calculus, along the SARAGO and CTD transects. Table 2 and figure 17 show the quantity (g) of chlorophyll *a* for both SARAGO and CTD casts. The values obtained clearly demonstrate an underestimation in the evaluation of quantities from CTD data, also in the areas strongly influenced by the frontal system. CTD quantities are always underestimated as regards SARAGO quantities. They vary, in fact, from 60 to 95%, with a mean of 89% of SARAGO quantities.

The highest chlorophyll *a* values, obtained from calculus with the SARAGO data, reflect the higher variability in the data structure allowing a finest quantification.

Table 2. Quantities of chlorophyll *a* (mg) calculated by the different methods in all the analysed transects

NP	Transect	Chl *a* quantity (g) by Trapezoidal	Chl *a* quantity (g) by Simpson	Chl *a* quantity (g) by Simpson3/8	Chl *a* quantity (g) by integral calculation	Area (m^2)
Sarago						
1	96 North Summer	171.873	171.72	171.878	171.873	800 000
2	96 South Summer	53.355	52.56	52.677	53.35	484 000
3	96 South Summer2	54.428	53.621	53.754	54.441	660 000
4	97 North Winter	536.834	537.136	536.994	536.867	625 000
5	97 South Winter	66.818	64.238	66.353	66.838	320 000
6	97 South Summer	107.226	105.545	105.598	107.231	750 000
CTD casts						
1	96 North Summer	130.723	130.687	130.666	130.733	800 000
2	96 South Summer	32.762	32.002	32.206	32.755	484 000
3	96 South Summer2	47.108	46.081	46.339	47.098	660 000
4	97 North Winter	468.727	468.319	468.355	468.832	625 000
5	97 South Winter	63.317	62.535	63.043	63.369	320 000
6	97 South Summer	76.528	74.67	74.801	76.623	750 000

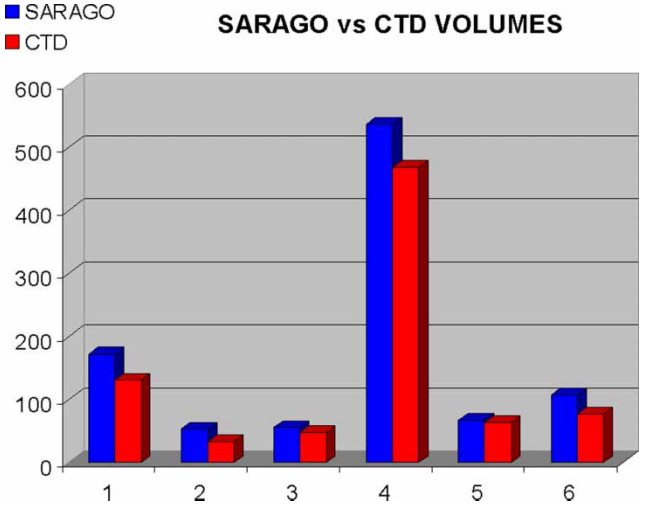

Figure 17. Graphical representation of SARAGO and CTD Chla quantity (g) by integral calculation.

During the PRISMA 2 cruises, the Primprod 1.11 was tested for the first time, installed on the SARAGO. In the intercalibration stations, the Primprod 1.08 (bought from the Biophysic Insitute of the Moscow University) and Primprod 1.11 were used simultaneously. This meant that the Primprod 1.11 could be tested with another pump and probe fluorometer.

The comparison between Primprod 1.11 and 1.08 gave very good results with an $r^2 = 0.9682$ (figure 18). The phyto VFP model was adapted to the structure of the SARAGO primary production data. Figure 19 shows the estimated primary production distribution, related to biomass and photosynthetic efficiency.

The density of information on chlorophyll *a* distribution makes it possible to estimate the primary production with a very high resolution. The primary production layout reflects the distribution both of the patchiness and of the other variables, considered in the model. The transect analysed was carried out from 11.30 to 13.30, in almost constant light conditions. The primary production calculus utilizes the PAR penetration, measured by SARAGO.

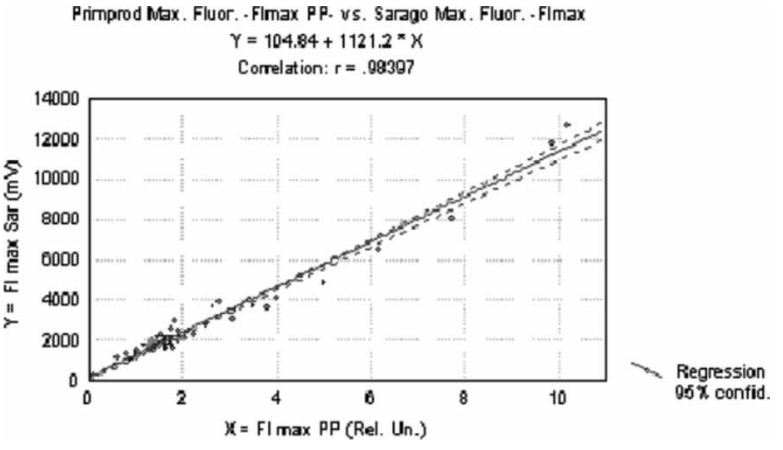

Figure 18. Regression between F_{max} measured by Primprod1.11 and F_{max} measured by Primprod1.08.

In the case studied here (figure 19), the primary production representation shows a self-shading area on the frontal zone. Inside the frontal system, evidenced by salinity distribution, the primary production is limited from the low PAR penetration due to the shade of upper layer phytoplanktonic population.

The upper-layer phytoplanktonic population limits the PAR penetration, thus inhibiting the primary production in the deepest layers. Also, the photosynthetic efficiency distribution reflects the light penetration. Inside the frontal area, the highest efficiency values are at a depth

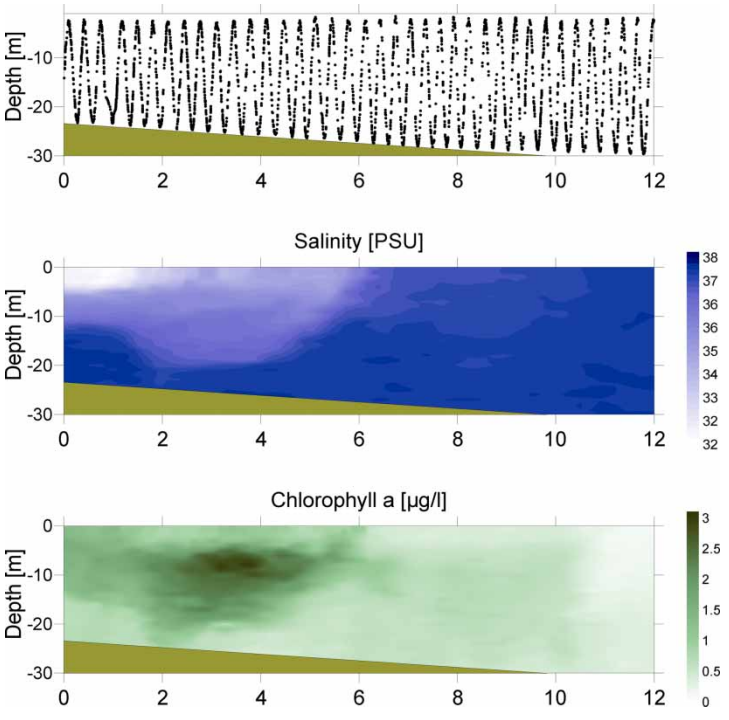

Figure 19. 1997 North Winter transect. Depth–distance sections. Top to bottom: SARAGO measure points; salinity (PSU); chlorophyll *a* (µ g l^{-1}); primary production (mg C^{-1} m^{-3} h^{-1}); photosynthetic efficiency (Rel. Un.).

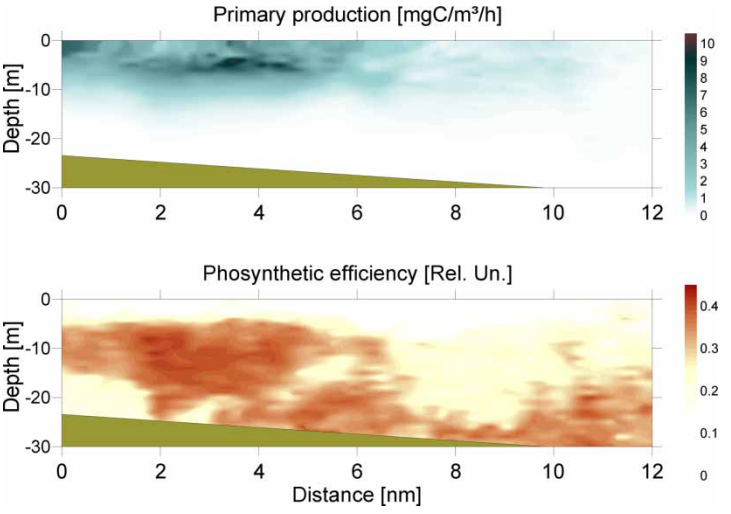

Figure 19. Continued.

of about 10 m, while outside the area, the highest values are at a depth of 20–30 m, because of a lower concentration of phytoplankton in the upper layer. This example emphasizes the quality and quantity of the informations that we can obtain from a high-resolution spatial and temporal analysis.

4. Discussion and conclusion

SARAGO allows data to be collected at a high temporal and spatial resolution: a profile is collected every ∼3 min (at a ship speed of 6 knots).

How important is this resolution in order to resolve the spatial and temporal variability of primary production? This paper tries to provide an answer.

From the representation of the variables in terms of maps, we observe fine structures, which traditional sampling methods cannot characterize because of the coarse sampling scheme of traditional CTD methods. Consequently, some structure, as chlorophyll patchiness of 600 m wide, are invisible to traditional methods.

Another cause of error is the time sampling period of CTD casts and the ecological and physical fluctuation timescales. The SARAGO solves this problem by reducing the length of the survey, that is than more than synoptic.

The variogram analysis shows that the SARAGO data do not present nugget effects in the variables analysed (temperature, salinity, and chlorophyll *a*), *i.e.* the sampling scheme solves the scales of the process. In contrast, the traditional sampling method always presents a high nugget effect value for chlorophyll *a*, and lower values for physical variables. The nugget effect of the CTD could be due to a lack of spatial and/or temporal resolution.

Both the platforms are equipped with a CTD SBE, with a flux system, with the difference that the CTD presents a more accurate instrument (SBE911) than SARAGO (SBE19); for this reason, we can exclude an instrumental error for the CTD casts nugget effects.

The high-resolution measurements of the SARAGO vehicle allowed the primary production and photosynthetic efficiency to be estimated for a portion of the Adriatic Sea, where self-shading effects could be important.

References

[1] M. Estrada, E. Berdalet. Phytoplankton in a turbulent world. *Sci. Mar.*, **61**(Suppl. 1), 125–140 (1997).
[2] R. Margalef. Environmental control of the mesoscale distribution of primary producers and its bearing to primary production in the western Mediterranean. In *Mediterranean marine ecosystems*, M. Moraiton-Apostopoulou, V. Kiostis (Eds), pp. 213–229, Plenum Press, New York (1985).
[3] J.H. Steel. *Spatial Pattern in Plankton Communities*, Plenum Press, New York (1978).
[4] V.H. Strass, Woods J.D. Horizontal and seasonal variation of density and chlorophyll profiles between Azores and Greenland. In Rothschild B.J. (Ed.) *Toward a Theory on Biological–Physical Interactions in the World Ocean*, B.J. Rothschild (Ed.), NATO ASI Series, pp. 113–137, Kluwer Academic, Dordrecht, Netherlands (1988).
[5] T.D. Dickey. Recent advances and future directions in multi-disciplinary in situ oceanographic measurements systems. In *Toward a Theory on Biological–Physical Interactions in the World Ocean*, B.J. Rothschild (Ed.), NATO ASI Series, pp. 555–599 Kluwer Academic, Dordrecht, Netherlands (1988).
[6] F. De Strobel, L. Gualdesi. High resolution towed oscillating system. *Sea Technol.*, *1994*, **35**, 37–40 (1994).
[7] A.W. Herman, T.M. Dauphinee. Continuous and rapid profiling of zooplankton with an electronic counter mounted on a 'Batfish' vehicle. *Deep-Sea-Res*., **27**, 79–96 (1980).
[8] M. Nomoto, Y. Tsuji, A. Misumi, T. Emura. An Advanced underwater towed vehicle for oceanographic measurements. *Adv. Underwat. Technol. Ocean Sci. Offshore Eng.*, **6**, 70–88 (1986).
[9] J. Aiken. The Undulating Oceanographic Recorder Mark 2′. *Plankton Res*., **3**, 551–560 (1981).
[10] F. Bahr, P. Fucile. Seasoar – a flying CTD. *Oceanus*, **38**, 26–28 (1995).
[11] M. Marcelli, E. Fresi. The Sarago Project. *Sea Technol.*, 62–67 (1997).
[12] G. Bortoluzzi, S. Cozzi, A. Di Maio, M. Marcelli. A method for surface and volume analysis of a 3-d function with an application to salinity data acquired by the tow-fish Sarago during cruises U1–U2–U3–U4 (prisma2 project, Adriatic Sea), IGM-CNR Cataloging-In-Publication data. In *TECHNICAL REPORT IGM-CNR*, 68.
[13] D. Bruzzi, M. Marcelli. Sviluppo di una metodologia strumentale automatica per il monitoraggio dei fondali marini. In *VI Colloquio AIOM* (Atti del Convegno), 79–84 (1990).
[14] P.G. Falkowski, Z. Kolber. Estimation of phytoplankton photosynthesis by active fluorescence. *ICES Mar. Sci. Symp.*, **197**, 92–103 (1993).
[15] T.K. Antal, P.S. Venediktov, D.N. Matorin, M. Ostrowska, B. Vozniak, A.B. Rubin. Measurement of phytoplankton photosynthesis rate using a pump and probe fluorometer. *Oceanologia*, **43** 291–313 (2001).
[16] U. Schreiber, H. Hormann, C. Neubauer, C. Klughammer. Assessment of photosystem II photochemical quantum yield by chlorophyll fluorescence quenching analysis. *Plant Physiol.*, **22** 209–220 (1995).
[17] JGOFS. Measurement of chlorophyll a and phaeopigments by fluorometric analysis. In *Protocols for the JGOFS core measurements (JGOFS Report Nr. 19). I.O.C. Manual and Guidelines*, Vol. 14, 119–122+Erratum (1994).
[18] L. Lazzara, F. Bianco, M. Falcucci, V. Hull, M. Modigh, M. Ribera d'Alcalà. Pigmenti clorofilliani. *Nova Thalassia*, **11**, 207–223 (1990).
[19] M.J. Fortin, M.R.T. Dale, J. ver Hoef. Spatial analysis in ecology. In *Encyclopedia of Environmetrics*, Vol. 4, A.H. El-Shaarawi, W.W. Piegorsch (Eds), pp. 2051–2058, Wiley, Chichester, UK (2002).
[20] A. Srivydia, E. Michael, M. Palaniyandy, S.P. Pani, P.K. Das. A geostatistical analysis of the geographic distribution of lymphatic filariasis prevalence in southern India. *Am. J. Trop. Med. Hygiene*, **67**, 480–489 (2002).
[21] M. Armstrong, *Basic Linear Geostatistics*, Springer, Berlin (1998).
[22] A. Journel, C. Huijbregts, *Mining Geostatistics*, Academic Press, London (1978).
[23] R. Barnes. The Variogram Sill and the Sample Variance. *Math. Geol.*, **23**, 673–678 (1991).
[24] M. Marcelli, O. Campana, A. Di Maio, O. Mangoni, M. Ribera D'alcala', V. Saggiomo, C. Tozzi, E. Fresi. Development of a new operative method to estimate primary production in the pelagic system with a quasi synoptic space time scale, paper presented at *Progress in Oceanography of the Mediterranean Sea International Conference*, Rome, 17–19 November, pp. 309–310 (1997).
[25] I. Nardello, L. Lazzara, M. Marcelli. Stime di biomassa e produzione primaria nel canale di Sicilia, attraverso misure di fluorescenza in vivo della clorofilla a. In *Proceedings of XIII Congresso nazionale della Società Italiana di Ecologia*, **27**, S11.8 (2003).
[26] J.T.O. Kirk. *Light and Photosynthesis in Aquatic Ecosystems*, Cambridge University Press, Cambridge (1983).
[27] D. Antoine, A. Morel. Oceanic primary production, 1. Adaptation of a spectral light-photosynthesis model in view of application to satellite chlorophyll observations. *Global Biogeochem. Cycles* **10**, 43–55 (1996).
[28] O. Mangoni, A. Bergamasco, F. Corato, V. Saggiamo. Variabilità spaziale dei processi do produzione primaria in un'area ad elevata instabilità idrografica: l'Adriatico settentrionale, *Atti XIII Congresso AIOL. Congresso nazionale della Società Italiana di Ecologia*, **27**, S11.8 (1998).
[29] E. Steeman Nielsen. The use of radioactive carbon (^{14}C) for measuring organic production in the sea. *J. Cons. Int. Explor. Mer.*, **18**, 117–140 (1952).
[30] W.H. Press, B.P. Flannery, S.A. Teukolsky, W.T. Vetterling. *Numerical Recipes in C*, Cambridge University Press, Cambridge (1988).